Published in final edited form as:
Neuroimage. 2014 November 15; 102(0 2): 729–735. doi:10.1016/j.neuroimage.2014.08.052.

Validation of the hypercapnic calibrated fMRI method using DOT-fMRI fusion imaging

Meryem A. Yücel[1,*], **Karleyton C. Evans**[2], **Juliette Selb**[1], **Theodore J. Huppert**[3], **David A. Boas**[1], and **Louis Gagnon**[1]

[1]MGH/HST Athinoula A. Martinos Center for Biomedical Imaging, Department of Radiology, Massachusetts General Hospital, Harvard Medical School, Charlestown, 02129, MA, USA

[2]Department of Psychiatry, Massachusetts General Hospital, Harvard Medical School, Charlestown, 02129, MA, USA

[3]Department of Radiology and Bioengineering, University of Pittsburgh, Pittsburgh, 15261, PA, USA

Abstract

Calibrated functional Magnetic Resonance Imaging (fMRI) is a widely used method to investigate brain function in terms of physiological quantities such as the cerebral metabolic rate of oxygen ($CMRO_2$). The first and one of the most common methods of fMRI calibration is hypercapnic calibration. This is achieved via simultaneous measures of blood-oxygenation-level dependent (BOLD) and the arterial spin labeling (ASL) signals during a functional task that evokes regional changes in $CMRO_2$. A subsequent acquisition is then required during which the subject inhales carbon dioxide for short periods of time. A calibration constant, typically labeled M, is then estimated from the hypercapnic data and is subsequently used together with the BOLD-ASL recordings to compute evoked changes in $CMRO_2$ during the functional task. The computation of M assumes a constant $CMRO_2$ during the CO_2 inhalation, an assumption that has been questioned since the origin of calibrated fMRI. In this study we used Diffuse Optical Tomography (DOT) together with BOLD and ASL – an alternative calibration method that does not require any gas manipulation and therefore no constant $CMRO_2$ assumption - to cross-validate the estimation of M obtained from a traditional hypercapnic calibration. We found a high correlation between the M values ($R=0.87$, $p<0.01$) estimated using these two approaches. The findings serve to validate the hypercapnic fMRI calibration technique and suggest that the inter-subject variability routinely

[*]Corresponding author: Meryem A. Yücel, Address: MGH/HST Athinoula A. Martinos Center for Biomedical Imaging, Department of Radiology, Massachusetts General Hospital, Harvard Medical School, 149, 13th street, Charlestown, 02129, MA, USA, Phone: 617 726 9338, mayucel@nmr.mgh.harvard.edu.

Conflict of interest

DB is an inventor on a technology licensed to TechEn, a company whose medical pursuits focus on noninvasive optical brain monitoring. DB's interests were reviewed and are managed by Massachusetts General Hospital and Partners HealthCare in accordance with their conflict of interest policies. KCE discloses grant support from Pfizer Ltd., unrelated to the present study.

obtained for M is reproducible with an alternative method and might therefore reflect inter-subject physiological variability.

Keywords

BOLD calibration; hypercapnia; fNIRS; $CMRO_2$

Introduction

The blood-oxygenation-level dependent (BOLD) contrast[1] in functional magnetic resonance imaging (fMRI) is a widely used tool to map brain activity. The technique rapidly found broad applications in basic neuroscience research[2] as well as in clinical studies[3]. Despite its widespread utilization, standard BOLD-fMRI is only a qualitative representation of brain activity[2]. The signal measured is a reflection of changes in cerebral blood flow (CBF) and cerebral metabolic rate of oxygen ($CMRO_2$), and also depends on baseline physiological parameters such as cerebral blood volume (CBV) and oxygen extraction fraction (OEF)[4,5,6,7]. This shortcoming of BOLD-fMRI significantly limits the interpretation of neural responses observed in between-group comparisons in clinical studies, particularly when individuals from clinical samples may have aberrant baseline physiology[8,9]. Thus, overcoming this drawback would enhance the utility of BOLD-fMRI for clinical investigations by facilitating unambiguous neuroimaging data in studies designed to test hypotheses related to pathophysiology within the human brain.

To overcome this problem, a significant effort has been directed towards estimating relative changes in $CMRO_2$ ($rCMRO_2$) from fMRI measurements. A method routinely used for this purpose is based on simultaneous measurements of the BOLD contrast together with a CBF measurement typically obtained from an arterial spin labeling (ASL) technique. In order to compute $rCMRO_2$ from the simultaneous BOLD-ASL acquisitions, the BOLD-ASL measurement is typically repeated during brief periods of carbon dioxide inhalation. This procedure has been referred to as BOLD calibration[5] and enables computation of a calibration constant for BOLD, which is routinely identified by the variable M in the literature[5,6].

An important assumption incorporated into the computation of M is that $CMRO_2$ remains constant during the hypercapnic challenge, an assumption that is still under debate. Some studies found no statistically significant change in $CMRO_2$ with a moderate increase in CO_2 levels[10,11,12], whereas other studies have found a significant decrease[13,14]. The discrepant findings in the literature combined with logistical and technical challenges involved with hypercapnic fMRI studies, has prompted the investigation of novel methods for calibrating the BOLD signal. Hyperoxic calibration[15], breath holding approach[16] and carbogen inhalation[17] are alternative approaches that also allow calibration of the BOLD signal. Although carbogen (any mixture of carbon dioxide and oxygen gas) inhalation still requires gas manipulation, it does not require constant $CMRO_2$. In this approach, it is aimed to obtain complete elimination of deoxyhemoglobin (HbR) by increasing arterial pO_2 and CBF, which provide a direct estimation of the M value. Finally, multimodal imaging combining

simultaneous diffuse optical tomography (DOT) and fMRI measurements[18,19,20] allows computation of M in the absence of gas manipulation or extra scans and all measurements are acquired simultaneously during the functional task of interest.

As the hypercapnic calibration is still the most commonly used method, there is a need for cross-validation of this technique against an alternative method. Ideally, the alternative method would not require a hypercapnic challenge or a critical assumption related to brain physiology. This will allow an independent consensus or dissent to the fMRI calibration literature. In the present study, M values obtained from the hypercapnic calibration procedure were cross-validated against those obtained with DOT-fusion model using simultaneous DOT-BOLD-ASL measurements.

Methods

Subjects

Eight healthy right-handed male subjects (26±5 years old) with no history of neurological, cardiopulmonary, or psychiatric illness participated in the study. All subjects were right-handed. The study was approved by the Partners Healthcare Human Subjects Committee and all subjects gave written consent form.

Experimental paradigm

The study comprised two imaging sessions conducted over a period of one hour: 1) four 6-min simultaneous acquisitions of: a) blood oxygen level dependent functional magnetic resonance imaging (BOLD-fMRI), b) arterial spin labeled (ASL)-fMRI and c) diffuse optical tomography (DOT) during a right hand finger tapping task, 2) two 10-min acquisitions of BOLD- and ASL-fMRI during hypercapnic challenge. The finger tapping task involved rapid opposition/touch of the thumb with the rest of the fingers. Each finger tapping scan included ~20 finger tapping trials of 10 sec duration with a pseudo-random inter-trial interval of 5–10 sec. Each hypercapnic challenge scan comprised alternating conditions of eucapnia (3 min) and hypercapnia (2 min) (3-min-off/2-min-on/3-min-off/2-min-on). During the hypercapnic condition, the inhalation gas was manually titrated to achieve an average increase in end-tidal CO_2 of 8 mmHg above each subject's baseline (habitual) end-tidal CO_2. A specialized breathing circuit was used to minimize breath to breath fluctuations in end-tidal CO_2 during the hypercapnic challenge scan[21] and thus mitigate associated artifacts[22].

DOT

A multichannel continuous wave optical imager (CW6, Techen Inc. Milford, Massachusetts) was used for this study. The instrument consisted of 32 lasers (half of them at 690 and the other half at 830 nm) and 32 detectors. Four sources and eleven detectors (eight long distance and three short distance) were used in this study. The DOT probe included one row of sources interleaved by short separation detectors[23], and two rows of long separation detectors above and below the source row. A fiducial marker was glued on top of each optode to determine the 3D locations in the anatomical MR volume. The probe was fixed on the left motor cortex of the subject during the finger tapping experiment. The probe was

removed during the gas manipulations to allow for more space in the coil for the gas mask. Optical density changes were obtained by taking the negative log of the light intensity. The sensitivity profiles were obtained running a GPU-bases Monte Carlo simulation (10^8 photons) on the segmented anatomical MPRAGE volume with five tissue layers. SPM software was used for segmentation (SPM8)[24].

Functional MR Imaging (BOLD and ASL)

Pulsed arterial spin labeled (pASL) sequence with proximal inversion with control for off-resonance effects (PICORE) labeling geometry[25] and thin-slice TI1 periodic saturation (Q2TIPS)[26] were obtained on a 3 T Siemens Trio MR Scanner (Siemens Medical Systems, Erlangen, Germany). Six slices of 6 mm thickness were acquired with the parameters: TR = 3 s, TE = 13 ms, TI1 = 600 ms, TI2 = 1800 ms, 3.4×3.4×6 mm resolution. A 3D anatomical volume was obtained using a T1-weighted MPRAGE sequence (1×1×1.33 mm resolution, TR/TE/α=2530 ms/3.25 ms/7°). The images were motion corrected and spatially smoothed with a 6-mm Gaussian kernel. The time courses were linearly interpolated. The BOLD time course images were obtained by combining the control images, whereas the perfusion time course images were obtained by iterative pair-wise subtraction of the tag images from the control images. The preprocessing steps above were performed using the FreeSurfer software[27].

Data Analysis

DOT-fusion model estimation of M—We used the DOT-BOLD-ASL fusion model described in Huppert et al., 2008[18] and Yücel et al., 2012[20] to simultaneously reconstruct oxy- and de-oxy hemoglobin (HbO and HbR) concentrations while simultaneously estimating the calibration constant M. A short description of the model is introduced here, details can be found in the references above. The model consisted of a linear model describing HbO and HbR spatio-temporal changes as well as three observation models relating HbO and HbR to changes in the DOT signal, BOLD signal and ASL signal respectively. The DOT observation model related the HbO and HbR changes to the light intensity change through the photon diffusion equation[28]. The BOLD observation model relied on the relationship between the BOLD signal and HbR signal[5]. For the ASL observation model, the Grubb relationship[29] was used to relate flow changes to total hemoglobin changes. Finally, the three observation models and the HbO and HbR models were concatenated in matrix form and then solved using a Bayesian formulation to reconstruct HbO and HbR changes as well as estimating the calibration constant M.

Hypercapnic estimation of M—We used the following equation[5] which assumes a constant $CMRO_2$ during the CO_2 challenge to estimate the M value:

$$M = \frac{B_H - 1}{1 - F_H^{-(\beta - \alpha)}} \quad \text{Eqn. 1}$$

The B_H and F_H are the BOLD and CBF ratio to baseline, β is a physical parameter (1.5)[5] and α is the Grubb's exponent (0.23)[30]. The subscript H indicates changes measured during the

hypercapnic challenge. When estimating the M value, we only used voxels with a statistically significant BOLD response over the motor and somatosensory areas of the contralateral cortex during the finger tapping task. The BOLD and CBF changes in the above-mentioned region of interest (ROI) were first averaged and then an estimate of the M value was obtained. As such, a single M value was obtained over the corresponding ROI.

$CMRO_2$ estimation—$CMRO_2$ was estimated by two different approaches: 1) using the M values obtained by hypercapnic calibration together with the BOLD and CBF data (Eqn.2) and 2) using the M values obtained from the fusion model and the BOLD, CBF and HbT data (Eqn.3)[5,31]. The symbol Δ indicates a change from baseline while the subscript 0 indicates baseline values.

$$\frac{\Delta CMRO_2}{CMRO_{2|0}} = \left(1 - \frac{\frac{\Delta BOLD}{BOLD_0}}{M}\right)^{1/\beta} \cdot \left(1 + \frac{\Delta CBF}{CBF_0}\right)^{1-\alpha/\beta} - 1 \quad \text{Eqn. 2}$$

$$\frac{\Delta CMRO_2}{CMRO_{2|0}} = \left(1 - \frac{\frac{\Delta BOLD}{BOLD_0}}{M}\right)^{1/\beta} \cdot \left(1 + \frac{\Delta HbT}{HbT_0}\right)^{-1/\beta} \cdot \left(1 + \frac{\Delta CBF}{CBF_0}\right) - 1 \quad \text{Eqn. 3}$$

Error Analysis—The error in M obtained from the hypercapnic calibration was estimated using Eqn. 4 where σ represents the variance[32], while the error in M obtained from the fusion model was estimated using Equations 5 and 6 where H is the fusion model forward matrix, *pinv* is the pseudo-inverse, and R is the measurement covariance[33]. For each method, error on $CMRO_2$ was estimated using Eqn. 7[32].

$$error_{M,hypercapnia} = \sqrt{\left(\frac{\partial M}{\partial BOLD}\right)^2 . \sigma^2_{BOLD} + \left(\frac{\partial M}{\partial CBF}\right)^2 . \sigma^2_{CBF}} \quad \text{Eqn. 4}$$

$$error_{M,fusion} = \sqrt{\left(\frac{\partial M}{\partial BOLD}\right)^2 . \sigma^2_{BOLD} + \left(\frac{\partial M}{\partial HbR}\right)^2 . \sigma^2_{HbR}} \quad \text{Eqn. 5}$$

$$\sigma^2_{HbR} = pinv(H)\, R\, pinv(H)^T \quad \text{Eqn. 6}$$

$$error_{CMRO_2} = \sqrt{\left(\frac{\partial CMRO_2}{\partial BOLD}\right)^2 . \sigma^2_{BOLD} + \left(\frac{\partial CMRO_2}{\partial CBF}\right)^2 . \sigma^2_{CBF} + \left(\frac{\partial CMRO_2}{\partial M}\right)^2 \cdot \sigma^2_M} \quad \text{Eqn. 7}$$

Results

Simultaneous recordings of DOT, BOLD and ASL during finger tapping and optical calibration of BOLD

Multimodal recordings of DOT, BOLD and ASL were performed simultaneously during a 10 s finger tapping task on 8 human subjects. All subjects showed significant BOLD, CBF and optical response to the finger tapping paradigm over the motor-sensory cortex (t statistics, $p<0.05$). Each subject was analyzed separately. Fig. 1A shows activation maps obtained using a standard GLM approach ($p<0.05$) for BOLD and CBF. Fig. 1B illustrates time courses of BOLD and CBF averaged over respective activation maps. Time courses of oxy- (HbO), deoxy- (HbR) and total hemoglobin (HbT) concentration changes measured simultaneously with DOT are plotted in Fig. 1C. The group average of the BOLD and CBF changes in response to finger tapping averaged over the ROI were 0.5% ± 0.2% (mean±std) and 40% ± 14% (mean±std) respectively.

For each subject, the complete data set (DOT, BOLD and ASL) was used in a multimodal fusion model to reconstruct changes in HbO and HbR and to simultaneously estimate the BOLD calibration constant M. This multimodal fusion model has been described in detail in our previous paper[20] and its key features are summarized in the *Methods* section. Fig. 2 shows the fusion model output for each of the eight subjects (HbO t-map, $p<0.05$). In each case, an increase in HbO and a decrease in HbR were reconstructed over the motor-sensory areas of the brain on the contralateral side to the finger tapping task. M values obtained from the fusion model are also shown for each subject and varied from 0.03 to 0.11.

BOLD and ASL responses to hypercapnia

For each subject, an extra scan was performed during which the subject breathed CO_2. We aimed to increase end-tidal pCO_2 ($EtCO_2$) by 8 mmHg in each run. Fig. 3A illustrates the time course of $EtCO_2$ for a typical subject. The resulting BOLD and CBF responses to hypercapnia averaged over trials and runs (two runs per each subject, each consisting of two trials of hypercapnia) are shown in Fig. 3B. For all subjects, hypercapnia led to global BOLD and CBF responses across the brain. The colored area in Fig. 3B corresponds to the six slices covered during the image acquisition. The group average of the BOLD and CBF changes during hypercapnia averaged over the same ROI were 1.4% ± 0.9% (mean±std) and 28% ± 23% (mean±std) respectively.

Inter-subject variability in M is consistent across both calibration techniques

The simultaneous BOLD-ASL acquisition during hypercapnia allowed for another estimation of the BOLD calibration constant M for each subject[5], independently of the one computed from the multimodal fusion model. Details of computations are provided in the *Methods* section.

The M values obtained with the hypercapnic calibration ranged from 0.03 to 0.11 across the 8 subjects (mean±std: 0.06 ±0.03). A subject-by-subject comparison of the M values obtained with each method is shown in Fig. 4 (see Table 1 for individual M values). A

correlation of R = 0.87 ($p < 0.01$) was obtained between the M values computed from the two methods.

The rCBF/$rCMRO_2$ ratio (also known as the flow-consumption ratio) was computed with both methods for each subject and values are presented in Table 2. A mean flow-consumption ratio of 1.5 ± 0.3 was obtained with the fusion model and a value of 1.8 ± 0.3 was obtained with the hypercapnic calibration. Such lower rCBF/$rCMRO_2$ values for the fusion model could potentially be explained by pial veins contamination in the NIRS data[34], which can results in slightly higher $rCMRO_2$ and therefore lower flow-consumption ratios. Moreover, both the fusion and the calibrated-fMRI flow-consumption values are slightly lower than the ones previously observed[35,36] for a finger tapping paradigm. A potential variability in finger tapping frequencies between different studies presented in the literature could explain this discrepancy[35].

The evoked changes in $CMRO_2$ in response to finger tapping recovered with each method were also compared and are shown in Table 2. A high correlation ($R = 0.98$, $p<0.01$) was obtained between the two methods. However, this high correlation between the changes in $CMRO_2$ should be carefully interpreted and probably arises from the shared noise, particularly ASL noise, between the two methods. In fact, the same BOLD and ASL signal acquired during finger tapping were used in the $CMRO_2$ calculation. However, it is important to note that this is not the case for the M value estimation, since different BOLD and ASL measurements were used to estimate M from the DOT-fusion model (the finger tapping measurements) and the hypercapnic calibration method (the hypercapnica measurements).

Discussion

In this study, we sought to validate the accuracy of the hypercapnic calibration of BOLD-fMRI by using an alternative approach that neither relies on gas manipulation nor an assumption of constant $CMRO_2$. For this purpose, the DOT-BOLD-ASL multimodal fusion[20] was the method of choice. A high degree of correlation was observed between the two methods for the calibration constant M ($R=0.87$, $p<0.01$). We contend that these data serve to cross-validate the hypercapnic calibration procedure and confirm its validity as a method to calibrate the BOLD signal and therefore extract $rCMRO_2$ time courses during a functional task.

We also aimed at investigating the origins of inter-subject variations in M values reported in the literature [15,37,38]. This inter-subject variability has been attributed to differences in baseline physiology across subjects but also to experimental noise. However, it has been difficult to quantify the fraction of the variability attributed to differences in baseline physiology because no alternative calibration method was used to test if the inter-subject variability was reproducible across different calibration modalities. Here, we found that the inter-subject variability in calibration constants M was consistent across the two calibration methods ($R = 0.87$, $p<0.01$). Moreover, the individual errors in M values (Table 2, Figure 4) were lower compared to the inter subject variability in M. These results taken together indicate that inaccuracies in the hypercapnic calibration procedure (i.e. experimental noise)

cannot account for a significant portion of the inter-subject variability. Therefore, differences in baseline physiology between subjects must account for most of the variability in M values.

Our group average values for M (Table 1) obtained with both modalities (6.6 ± 2.8 for the fusion model and 5.9 ± 2.5 for the hypercapnic calibration) are comparable with previously published values obtained over the motor cortex (4.3 ± 3.5[36], 6.1 ± 1.1[35]). The intra-subject variability in M reported in Table 1 is also comparable with literature[32] and ranges between <0.1 and 1.7 % for the fusion model and between 0.4 and 1.9 % for the hypercapnic calibration.

Estimation of the M value could be biased by some assumed parameters in the model, as discussed previously in our previous paper[20]. However, our analysis showed that variation in the baseline oxygen extraction fraction was not sufficient to explain the variability in M values across subjects[20]. As for the Grubb's constant (α) and the imaging parameter β, we used the same values in the two calibration methods. This procedure decreases their contribution as a source of variability in the comparison of the M values.

A non-negligible rCBF and hence $rCMRO_2$ variability was observed between subjects which could be the result of variability in the finger tapping frequencies between different subjects. Previous work has shown that the magnitude of the hemodynamic response depends on the frequency of finger tapping.[35, 39] In this work, the frequency of finger tapping was not controlled, and thus this maybe a confounding factor in the variability in $rCMRO_2$. The noise in ASL measurements is another factor that can further add up to this variability.

The choice of the ROI is also a source of variation in the $rCBF/rCMRO_2$ ratio estimation[37]. In this study, we chose the ROIs based on voxels with significant BOLD activation during the finger tapping runs. BOLD was selected over ASL because of its higher signal-to-noise ratio. Although it does not change our main results, it is still important to discuss the effect of using an ASL-based or an overlapping BOLD and ASL based ROI instead. Our estimation of $CMRO_2$ using an ASL-based ROI as well as an overlapping BOLD and ASL based ROI (not shown) tend to be higher compared to $CMRO_2$ calculated using a BOLD-based ROI, with the ASL-based ROI giving the highest values. This was due to the fact that the CBF change in ASL-based ROI was higher than that in BOLD based ROI, as would be expected. The corresponding M values decreased due to the same reason i.e. the higher CBF. We note that the M values obtained from fusion model were independent of the ROI selection.

The interpretations of the present study should be considered on balance with certain limitations. Although our two different $rCMRO_2$ estimations relied on two independent calibration constants, they both depended upon a simplified form of the Davis model[5]. Consequently, a systematic bias introduced by this simplification may not have been detected in the current work. Although other cross-validation approaches such as PET would avoid this potential confound, resources for the current study precluded the inclusion of PET imaging. Nevertheless, the constant inter-subject variability across modalities observed in

the present study serves as robust and convincing evidence to support the hypercapnic fMRI technique in calibration of the BOLD signal.

Acknowledgments

We would like to thank Jean J Chen, Divya Bolar, Donald Mclaren and Elfar Adalsteinsson for helpful discussions regarding the analysis performed in this work. We also thank Richard Hoge, Frederic Lesage, Bruce Rosen and Claudine Gauthier for their guidance in initiating this project. We wish to also acknowledge Tian Yue, Allison Song and Jared Zimmerman for technical assistance. Primary support for this work was P41-RR14075 and R01-EB0000790. This work was supported in part by K23MH086619 (KCE).

References

1. Ogawa S, Lee TM, Kay AR, Tank DW. Brain magnetic resonance imaging with contrast dependent on blood oxygenation. Proc Natl Acad Sci U S A. 1990; 87:9868–9872. [PubMed: 2124706]
2. Logothetis NK. What we can do and what we cannot do with fMRI. Nature. 2008; 453:869–878. [PubMed: 18548064]
3. Matthews PM, Honey GD, Bullmore ET. Applications of fMRI in translational medicine and clinical practice. Nat Rev Neurosci. 2006; 7:732–744. [PubMed: 16924262]
4. Buxton RB, Wong EC, Frank LR. Dynamics of blood flow and oxygenation changes during brain activation: the balloon model. Magn Reson Med. 1998; 39:855–864. [PubMed: 9621908]
5. Davis TL, Kwong KK, Weisskoff RM, Rosen BR. Calibrated functional MRI: mapping the dynamics of oxidative metabolism. Proc Natl Acad Sci USA. 1998; 95:1834–1839. [PubMed: 9465103]
6. Hoge RD, et al. Investigation of BOLD signal dependence on cerebral blood flow and oxygen consumption: the deoxyhemoglobin dilution model. Magn Reson Med. 1999; 42:849–863. [PubMed: 10542343]
7. Kim S-G, Ogawa S. Biophysical and physiological origins of blood oxygenation level-dependent fMRI signals. J Cereb Blood Flow Metab. 2012; 32:1188–1206. [PubMed: 22395207]
8. Buxton RB. Interpreting oxygenation-based neuroimaging signals: the importance and the challenge of understanding brain oxygen metabolism. Front Neuroenergetics. 2010; 2:8. [PubMed: 20616882]
9. Hoge RD. Calibrated FMRI. Neuroimage. 2012; 62:930–937. [PubMed: 22369993]
10. Kety SS, Schmidt CF. The effects of altered arterial tensions of carbon dioxide and oxygen on cerebral blood flow and cerebral oxygen consumption of normal young men. J Clin Invest. 1948; 27:484–492. [PubMed: 16695569]
11. Sicard KM, Duong TQ. Effects of hypoxia, hyperoxia, and hypercapnia on baseline and stimulus-evoked BOLD, CBF, and CMRO2 in spontaneously breathing animals. Neuroimage. 2005; 25:850–858. [PubMed: 15808985]
12. Chen JJ, Pike GB. MRI measurement of the BOLD-specific flow-volume relationship during hypercapnia and hypocapnia in humans. Neuroimage. 2010; 53:383–391. [PubMed: 20624474]
13. Xu F, et al. The influence of carbon dioxide on brain activity and metabolism in conscious humans. J Cereb Blood Flow Metab. 2011; 31:58–67. [PubMed: 20842164]
14. Bolar DS, Rosen BR, Evans KC, Sorenson AG, Adalsteinsson E. Depression of cortical gray matter $CMRO_2$ in awake human during hypercapnia. Proc Intl Soc Mag Reson Med. 2010:18.
15. Chiarelli PA, Bulte DP, Wise R, Gallichan D, Jezzard P. A calibration method for quantitative BOLD fMRI based on hyperoxia. Neuroimage. 2007; 37:808–820. [PubMed: 17632016]
16. Kastrup A, Krüger G, Glover GH, Moseley ME. Assessment of cerebral oxidative metabolism with breath holding and fMRI. Magn Reson Med. 1999; 42:608–611. [PubMed: 10467308]
17. Gauthier CJ, Madjar C, Tancredi FB, Stefanovic B, Hoge RD. Elimination of visually evoked BOLD responses during carbogen inhalation: implications for calibrated MRI. Neuroimage. 2011; 54:1001–1011. [PubMed: 20887792]
18. Huppert TJ, Diamond SG, Boas DA. Direct estimation of evoked hemoglobin changes by multimodality fusion imaging. J Biomed Opt. 2008; 13:054031. [PubMed: 19021411]

19. Tak S, Jang J, Lee K, Ye JC. Quantification of CMRO(2) without hypercapnia using simultaneous near-infrared spectroscopy and fMRI measurements. Phys Med Biol. 2010; 55:3249–3269. [PubMed: 20479515]
20. Yücel MA, Huppert TJ, Boas DA, Gagnon L. Calibrating the BOLD signal during a motor task using an extended fusion model incorporating DOT, BOLD and ASL data. Neuroimage. 2012; 61:1268–1276. [PubMed: 22546318]
21. Banzett RB, Garcia RT, Moosavi SH. Simple contrivance "clamps" end-tidal PCO(2) and PO(2) despite rapid changes in ventilation. J Appl Physiol. 2000; 88:1597–1600. [PubMed: 10797118]
22. Wise RG, Ide K, Poulin MJ, Tracey I. Resting fluctuations in arterial carbon dioxide induce significant low frequency variations in BOLD signal. Neuroimage. 2004; 21:1652–1664. [PubMed: 15050588]
23. Gagnon L, et al. Improved recovery of the hemodynamic response in diffuse optical imaging using short optode separations and state-space modeling. Neuroimage. 2011; 56:1362–1371. [PubMed: 21385616]
24. Ashburner, J.; Friston, KJ. Image segmentation. In: Frackowiak, RSJ.; Friston, KJ.; Frith, C.; Dolan, R.; Friston, KJ.; Price, CJ.; Zeki, S.; Ashburner, J.; Penny, WD., editors. Human Brain Function. 2. Academic Press; 2003.
25. Wong EC, Buxton RB, Frank LR. Implementation of quantitative perfusion imaging techniques for functional brain mapping using pulsed arterial spin labeling. NMR Biomed. 1997; 10:237–249. [PubMed: 9430354]
26. Luh WM, Wong EC, Bandettini PA, Hyde JS. QUIPSS II with thin-slice TI1 periodic saturation: a method for improving accuracy of quantitative perfusion imaging using pulsed arterial spin labeling. Magn Reson Med. 1999; 41:1246–1254. [PubMed: 10371458]
27. Dale AM, Fischl B, Sereno MI. Cortical surface-based analysis. I. Segmentation and surface reconstruction. Neuroimage. 1999; 9:179–194. [PubMed: 9931268]
28. Dehghani H, Delpy DT, Arridge SR. Photon migration in non-scattering tissue and the effects on image reconstruction. Phys Med Biol. 1999; 44(12):2897–2906. [PubMed: 10616143]
29. Grubb RL Jr, Raichle ME, Eichling JO, Ter-Pogossian MM. The effects of changes in PaCO2 on cerebral blood volume, blood flow, and vascular mean transit time. Stroke. 1974; 5:630–639. [PubMed: 4472361]
30. Chen JJ, Pike GB. BOLD-specific cerebral blood volume and blood flow changes during neuronal activation in humans. NMR Biomed. 2009; 22:1054–1062. [PubMed: 19598180]
31. Lin A-L, et al. Time-dependent correlation of cerebral blood flow with oxygen metabolism in activated human visual cortex as measured by fMRI. Neuroimage. 2009; 44:16–22. [PubMed: 18804541]
32. Mark CI, Pike GB. Indication of BOLD-specific venous flow-volume changes from precisely controlled hyperoxic vs. hypercapnic calibration. JCBFM. 2012; 32(4):709–19.
33. Ye JC, Tak S, Jang KE, Jung J, Jang J. NIRS-SPM: statistical parametric mapping for near-infrared spectroscopy. Neuroimage. 2009; 44(2):428–47. [PubMed: 18848897]
34. Gagnon L, et al. Quantification of the cortical contribution to the NIRS signal over the motor cortex using concurrent NIRS-fMRI measurements. Neuroimage. 2012; 59:3933–3940. [PubMed: 22036999]
35. Stefanovic B, Warnking JM, Rylander KM, Pike GB. The effect of global cerebral vasodilation on focal activation hemodynamics. Neuro Image. 2006; 30:726–734. [PubMed: 16337135]
36. Chiarelli PA, et al. Flow-metabolism coupling in human visual, motor, and supplementary motor areas assessed by magnetic resonance imaging. Magn Reson Med. 2007; 57:538–547. [PubMed: 17326178]
37. Leontiev O, Buxton RB. Reproducibility of BOLD, perfusion, and CMRO2 measurements with calibrated-BOLD fMRI. Neuroimage. 2007; 35:175–184. [PubMed: 17208013]
38. Kastrup A, Krüger G, Neumann-Haefelin T, Glover GH, Moseley ME. Changes of cerebral blood flow, oxygenation, and oxidative metabolism during graded motor activation. Neuroimage. 2002; 15(1):74–82. [PubMed: 11771975]
39. Riecker A, Wildgruber D, Mathiak K, Grodd W, Ackermann H. Parametric analysis of rate-dependent hemodynamic response functions of cortical and subcortical brain structures during

auditorily cued finger tapping: a fMRI study. Neuroimage. 2003; 18(3):731–9. [PubMed: 12667850]

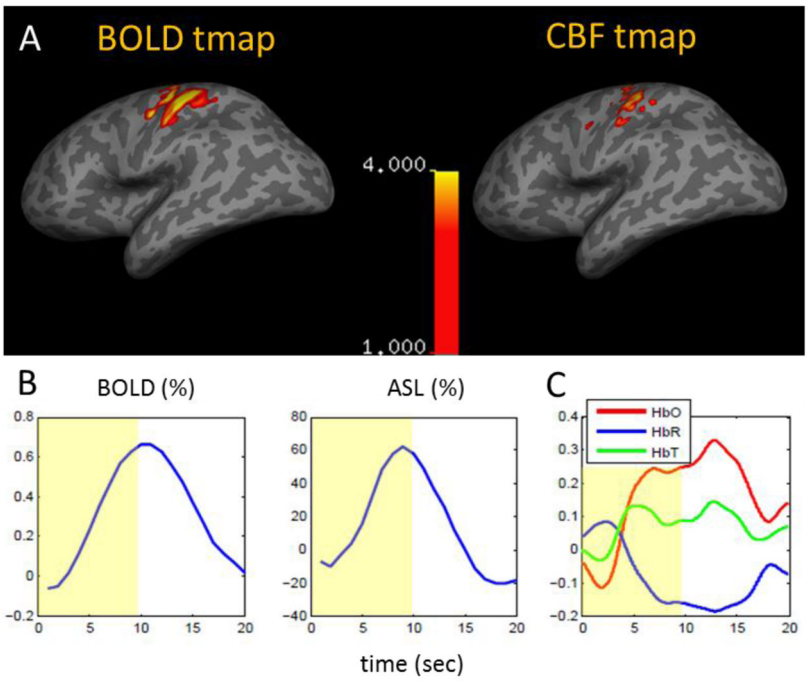

Figure 1.

Multimodal recordings of BOLD, ASL and DOT for a typical subject. A) Activation maps ($p<0.05$) for BOLD and CBF respectively. B) BOLD and CBF responses averaged over its respective statistically significant voxels. C) HbO (red), HbR (blue) and HbT (green) (μM) responses from simultaneous DOT recordings.

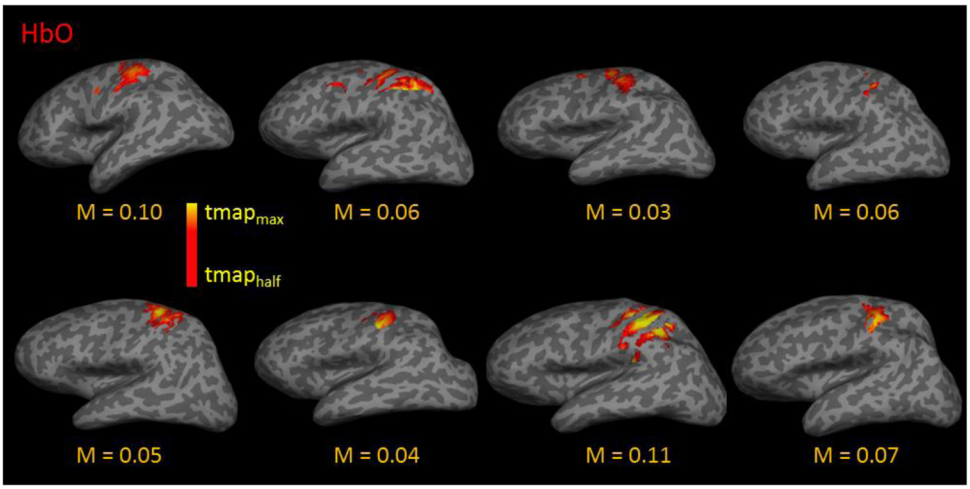

Figure 2.

Output of the DOT-BOLD-ASL multimodal fusion model. HbO t-maps ($p<0.05$) are shown for each subject (n=8). Activation was reconstructed over the motor and somatosensory regions. The fusion model also simultaneously estimate the BOLD calibration constant M, which is given for each subject.

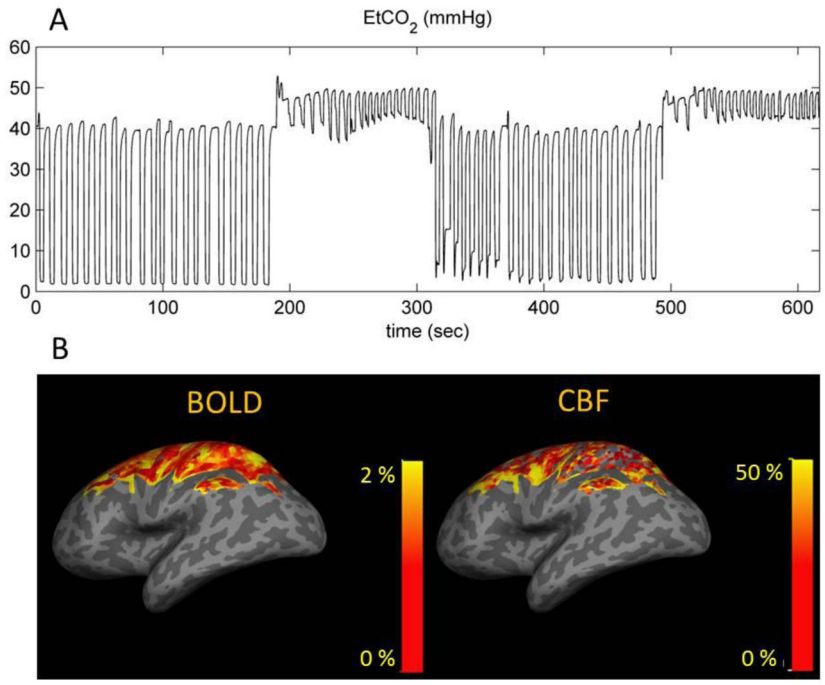

Figure 3.

Simultaneous BOLD and ASL measurement during hypercapnia. A) End-tidal pCO_2 ($EtCO_2$) (mmHg) time course during a hypercapnic challenge (example data from a typical subject). An increase of 8 mmHg was aimed for $EtCO_2$ during the hypercapnic inhalation. B) Percent signal change in BOLD and CBF responses to hypercapnia for a typical subject. The colored area corresponds to the six slices covered during the image acquisition.

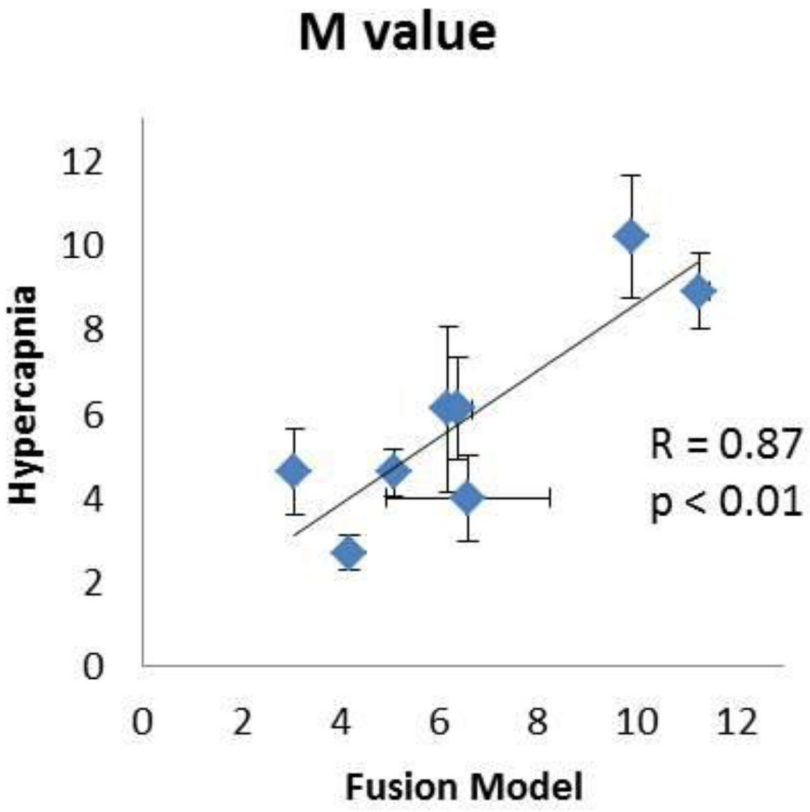

Figure 4.
Comparison of M values (in percent) obtained using the multimodal DOT-BOLD-ASL fusion model against those obtained from the hypercapnic calibration (n=8).

Table 1

M values from the fusion model and the hypercapnic calibration (mean ± standard error).

Subject	M_{fusion}	$M_{hypercapnia}$
1	9.9 ± 0.1	10.2 ± 1.4
2	6.2 ± 0.0	6.1 ± 1.9
3	3.1 ± 0.0	4.6 ± 1.0
4	6.4 ± 0.3	6.1 ± 1.2
5	5.1 ± 0.1	4.6 ± 0.6
6	4.2 ± 0.1	2.7 ± 0.4
7	11.3 ± 0.2	8.9 ± 0.9
8	6.6 ± 1.7	4 ± 1.0
Mean + Std	6.6 ± 2.8	5.9 ± 2.5

Table 2

BOLD response, CBF response, Flow-consumption ratios (n=rCBF/rCMRO$_2$), and CMRO$_2$ changes (all in percent) measured during finger tapping, (mean ± standard error).

Subject	BOLD	CBF	n_{Fusion}	$n_{Hypercapnia}$	$CMRO_{2,fusion}$	$rCMRO_{2,hypercapnia}$
1	0.66 ± 0.04	62 ± 3	1.2	1.4	50 ± 2	44.0 ± 3
2	0.50 ± 0.03	45 ± 2	1.2	1.5	37 ± 2	29.4 ± 3
3	0.40 ± 0.02	53 ± 3	1.4	1.5	38 ± 3	35.0 ± 3
4	0.80 ± 0.16	45 ± 3	1.4	1.8	32 ± 3	24.8 ± 4
5	0.66 ± 0.06	31 ± 2	2.2	2.3	14 ± 2	13.4 ± 2
6	0.35 ± 0.03	36 ± 3	1.5	2.0	25 ± 2	18.2 ± 3
7	0.54 ± 0.05	26 ± 2	1.5	1.6	17 ± 1	16.7 ± 2
8	0.31 ± 0.03	19 ± 3	1.6	1.9	12 ± 2	9.8 ± 3
Mean + Std	0.53 ± 0.17	40 ± 14	1.5 ± 0.3	1.8 ± 0.3	28 ± 13	24 ± 12